Indian Journal of Chemistry
Vol. 65, April 2026, pp. 337-347
DOI: 10.56042/ijc.v65i4.24654

A biophysical study of Ru(II) polypyridyl complexes of 2-(4-(pyrimidine-5-yl)phenyl)-1*H*-imidazo[4,5-f][1,10]phenanthroline [NPPIP] ligand, its DNA binding affinity and biological activity

Navaneetha Nambigari*[a,b] & Markandeya Namani[a]

[a] Department of Chemistry, University College of Science, Saifabad, Osmania University, Hyderabad 500 004, Telangana State, India
[b] Department of Chemistry, University College of Science, Osmania University, Tarnaka, Hyderabad 500 007, Telangana State, India
E-mail: nitha379@gmail.com, navaneeta@osmania.ac.in

Received 9 October 2025; accepted (revised) 3 March 2026

Ru(II) polypyridyl complexes of $[Ru(A)_2NPPIP]$ $(ClO_4)_2.2H_2O$, where NPPIP = 2-(4-(pyrimidine-5-yl)phenyl)-1*H*-imidazo[4,5-f][1,10]phenanthroline and A = phen = (1,10-phenanthroline)(1), bpy = bipyridine(2) and dmb = 4,4'-dimethyl-2,2'-bipyridine(3), have been synthesized and characterized using various spectroscopic techniques. The interaction of these complexes with DNA has been studied using biophysical methods, including absorption, emission, and viscosity measurements. The results indicate that the Ru(II) polypyridyl complex binds to DNA primarily through intercalation. Among the complexes, the phen complex exhibits the strongest DNA binding affinity, followed by bpy and dmb, highlighting the influence of the ancillary ligand on DNA binding specificity. This has been further confirmed by the binding constants (K_b), which have been determined to be 2.5×10^5 M^{-1}(from UV-Vis absorption) and 7.2×10^6 M^{-1}(from fluorescence emission studies), and the Stern-Volmer quenching constant (K_{sv}), which was 9.2×10^3. Antimicrobial studies on Gram-negative (*E. coli* and *K. pneumoniae*) and Gram-positive (*S. aureus* and E. *faecalis*) bacteria show significant activity. Additionally, the anti-cancer potential of the complexes has been evaluated using the MTT assay against the MCF-7 cell line, demonstrating strong anticancer activity correlated with their DNA binding properties.

Keywords: Ru(II) polypyridyl complexes, DNA binding, Binding constant, Antimicrobial, Anticancer

The discovery of *cis*-platin's antitumor properties in the mid-1960s revolutionised cancer chemotherapy. Today, *cis*-platin, carboplatin, and oxaliplatin are widely used platinum-based chemotherapeutic agents[1]. However, issues such as side effects, drug resistance, and limited action prompted ongoing research for new transition metal complexes with anticancer potential[2]. Ru complexes have received a lot of interest in inorganic chemistry during the last four decades because of their distinct biological, catalytic, optical, and electrical features[3-9]. Ru complexes have several advantages in drug development, including: (i) multiple accessible oxidation states (II, III, IV) at physiological *p*H, which influences drug distribution, (ii) slow ligand-exchange kinetics similar to Pt complexes, (iii) well-established coordination chemistry, (iv) lower toxicity than Pt-based drugs, and (v) coordination properties similar to Fe[10-13]. An advantage of Ru(II) complexes is their tunable photophysical properties, desirable for photoactivated biological applications.

Additionally, the octahedral geometry of Ru complexes allows chemists to create molecules with complex three-dimensional structures[14]. As a result, these complexes have found growing applications in supramolecular chemistry and, notably, in biological systems. They have been used to explore non-covalent binding interactions with DNA and as luminescent probes[15-18]. The distinct photophysical properties of ruthenium complexes compel as DNA probes, cellular imaging, protein monitoring, and anticancer activity. Presently, three Ru(III) complexes have entered clinical trials, showing potential advantages such as (i) reduced toxicity compared to Pt-based drugs, (ii) transferrin-mediated delivery into cells, and (iii) reduction to the Ru(II) ion ("activation-by-reduction") under hypoxic tumour conditions. These include NKP-1339 (sodium salt of *trans*-[tetrachlorobis(1H-indazole)-ruthenate(III)]), KP-1019 (indazolium salt of *trans*-[tetrachlorobis(1H-indazole)-ruthenate(III)]), and NAMI-A (imidazolium *trans*-[tetrachloro(dimethylsulfoxide)(1H-imidazole)-

ruthenate(III)]). Recently, the Ru(II) polypyridyl complex TLD-1433 has also entered clinical trials[19-25].

Drug-resistant bacteria have become a global health problem, resulting in a renewed effort to discover antibiotics with novel mechanisms of action.Initial research on the antimicrobial activity of Ru(II) polypyridyl complexes, such as $[Ru(Me_4phen)_3]^{2+}$, was carried out by Dwyer *et al*. The mononuclear $[Ru(phen)_3]^{2+}$ complex showed no antimicrobial activity against Gram positive and Gram-negative bacteria[26,27]. The interaction of antimicrobial agents with DNA is postulated in many publications as a potential mode of action. Bolhuis *et al*. described the results for three compounds employing different intercalating ligands with different DNA affinities– dpq, dpqC and dppz[28].

Srishailam *et al*. discovered a similar association between DNA binding affinity and antibacterial activity for a range of Ru complexes[29]. In this investigation, the highest antibacterial activity was connected with the highest DNA binding affinity and cleavage activity. Modifying the coordination sphere of Ru-arene complexes led to the formation of promising potential anticancer compounds with an unconventional mechanism of action. Hence, there is a continuous need for establishing new classes of antimicrobial drugs to prevent the spread of bacterial immune strains.

In this study, the ligand NPPIP [2-(4-(pyrimidine-5-yl)phenyl)-1H-imidazo[4,5-f][1,10]phenanthroline] and its Ru(II) metal complex were synthesized and characterized using IR, UV, ^{1}H and ^{13}C NMR, mass spectrometry, and elemental analysis. The interaction of the complex with CT-DNA was investigated using UV-Visible absorption titration, fluorescence emission, and viscosity tests. The combination successfully cleaved the plasmid pBR322 DNA. The compound was also tested for its antibacterial and cytotoxic properties.

Experimental Section

The required reagents were of analytical grade and used as received unless otherwise specified. 1,10-Phenanthroline monohydrate (phen), 2,2'-bipyridine (bpy), 4,4'-dimethyl-2,2'-bipyridine (dmb), $RuCl_3 \cdot 3H_2O$, dimethyl sulfoxide, and CT-DNA were purchased from Sigma-Aldrich. Supercoiled pBR322 plasmid DNA (stored at -20°C) was obtained from Fermentas Life Sciences, and agarose gel was purchased from Genei. All other chemicals and solvents were sourced locally and used without further purification. Solvents were purified prior to use according to standard procedures. Ultrapure Milli-Q water (18.2 MΩ) was used for all experiments. Tris buffer (*p*H 7.2) was prepared in double-distilled water using 5 mmol Tris-HCl and 50 mmol NaCl for studying the binding affinity of the complexes with CT-DNA.

Elemental analyses for C, H, and N were conducted using a PerkinElmer 240 analyzer. ^{1}H and ^{13}C NMR spectra were recorded on a Bruker 400/DRX spectrometer using DMSO-d_6 as the solvent. Infrared spectra were obtained on a PerkinElmer 1605 FTIR spectrometer with KBr disks. UV–Vis spectra were recorded on a Shimadzu UV-2600 spectrophotometer, and luminescence spectra were obtained using a Cary Eclipse spectrofluorometer (serial number MY12400004) to calculate the binding constant. Viscosity measurements were carried-out with an Ostwald viscometer. Mass spectra were recorded using a Quattro LC triple quadrupole mass spectrometer, equipped with Mass Lynx software (Micromass, Manchester, UK).

CT-DNA, obtained from Sigma-Aldrich, was used as received. The concentration of CT-DNA solutions was determined spectrophotometrically using a molar absorptivity of ε_{660} nm = 0.66×10^4 M^{-1} cm^{-1}. The CT-DNA solution in Tris–HCl buffer showed a UV absorbance ratio of $\lambda_{260}/\lambda_{280} \geq 1.9$, confirming that the DNA was protein-free. Stock solutions of CT-DNA were prepared in buffer (UV absorbance at 260 nm after 1:20 dilution) and stored at 4°C for no longer than four days. A stock solution of metal complexes was prepared by dissolving the required amounts in DMSO and diluting to the necessary concentrations for the experiments with the appropriate buffer[30,31].

Synthesis of NPPIP ligand and its Ru(II) complexes

The 2-(4-(pyrimidine-5-yl)phenyl)-1H-imidazo [4,5-f][1,10]phenanthroline [NPPIP] ligand was synthesized using phendione (0.53g, 2.5mmol), 4-(pyrimidin-5-yl)benzaldehyde (0.644g, 3.5 mmol), and ammonium acetate (3.86 g, 50 mmol). These components were dissolved in glacial acetic acid (15 mL) and refluxed for 5 hours (Scheme 1)[32,33]. A distinct brick-red solution was obtained, which was cooled to RT and transferred to distilled water. Concentrated ammonia (NH_3) was then added dropwise, resulting in the formation of an orange-

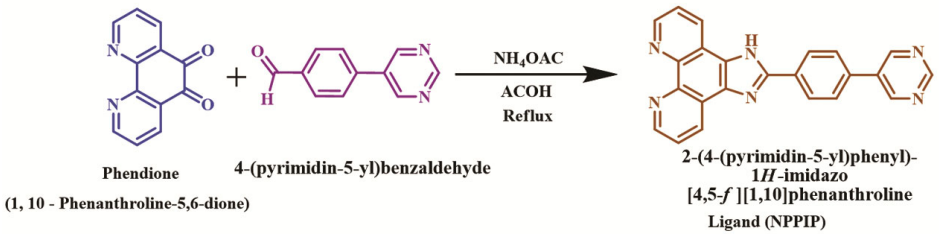

Scheme 1 — Synthesis of NPPIP ligand

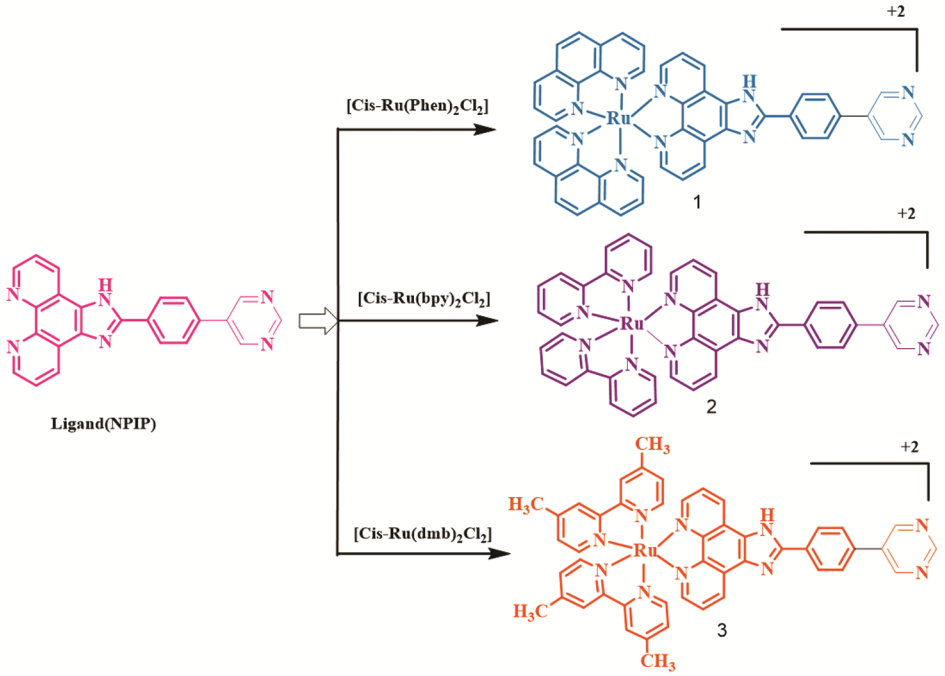

Scheme 2 — Synthesis of Ruthenium polypyridyl complexes, $[Ru(phen)_2NPPIP]^{+2}$ (**1**) $[Ru(bpy)_2NPPIP]^{+2}$(**2**) and $[Ru(dmb)_2NPPIP]^{+2}$(**3**)

yellow precipitate. The precipitate was collected, washed with water, and dried. The crude product was recrystallised using ethanol-water (C_2H_5OH/H_2O) and dried. Furthermore, the ligand was used in the synthesis of various Ruthenium complexes, named as complex-1, complex-2, and complex-3. And their spectra are given in Supplementary Information (Figure S2 - Figure S17). Analytical data: Calcd for $C_{23}H_{14}N_6$: C, 73.78; H, 3.77; N, 22.45. Found: C, 73.79; H, 3.79; N, 22.47%. ESI-MS: *m/z* Calcd 374.1. Found 375.2; ^{1}H NMR (DMSO-d_6, 400 MHz): δ 13.95 (s, 1H), 9.30 (s, 2H), 9.25 (s, 1H), 9.06 (dd, 2H), 8.98 (d, 2H), 8.46 (d, 2H), 8.11 (d, 2H), 7.87 (d, 2H); ^{13}C[^{1}H] NMR (100, MHz, DMSO-d_6): δ 172.04, 157.45, 154.66, 149.91, 147.26, 134.44, 132.39, 130.21, 127.33, 123.20; IR (KBr): 3444 (υ,N-H), 2924 (υ,C-H), 1188 (υ,C-N), 1695 (υ,C=C), 1570 cm^{-1} (υ,C=N). Yield 68%.

Synthesis of $[Ru(phen)_2(NPPIP)](ClO_4)_2.2H_2O$, 1

A solution of *cis*-$[Ru(phen)_2Cl_2]\cdot 2H_2O$ (0.5 mmol, 0.284 g) and NPPIP ligand (0.5 mmol, 0.187 g) in ethanol (15 mL) was refluxed at 120°C for 14 hours with a nitrogen purge. After cooling the light purple solution to ambient temperature, a saturated aqueous $NaClO_4$ solution was vigorously stirred in. The resultant crimson solution was collected, rinsed with diethyl ether, ethanol, and water, and then hoover dried. Yield: 62.7% (Scheme 2). Analytical data: Calcd for $C_{47}H_{30}N_{10}Ru$: C, 67.53; H, 3.62; N, 16.76. Found: C, 67.55; H, 3.66; N, 16.78%. ^{1}H NMR (DMSO-d_6 ,400 MHz): δ 9.28 (d, 3H), 9.24 (d, 3H), 9.07 (d, 3H), 9.04 (m, 3H), 8.78 (d, 2H), 8.45 (s, 2H), 8.38 (m, 2H), 8.11 (m, 3H), 8.08 (m, 3H), 7.97 (t, 2H), 7.78 (d, 2H), 7.75 (m, 2H); ^{13}C[^{1}H] NMR(100, MHz, DMSO-d_6): δ 157.09, 154.66, 152.75, 150.10, 141.38, 136.79, 134.61, 132.32, 130.42, 127.33,

126.91, 123.90; IR (KBr): 3534 (υ, N-H), 2925 (υ, C-H), 1089 (υ, C-N), 1555(ϑ, C=N), 1739 (υ, C=C), 623 cm^{-1} (υ, Ru-N).

Synthesis of $[Ru(bpy)_2(NPPIP)](ClO_4)_2.2H_2O$ (2)

By following the complex-1 procedure, we synthesised $[Ru(bpy)_2(NPPIP)]^{+2}$**(2)** complex by adding a mixture of *cis*-$[Ru(bpy)_2Cl_2]\cdot 2H_2O$ (0.5 mmol, 0.26 g) and NPPIP ligand (0.5 mmol, 0.187 g) was prepared in ethanol (15 mL). Analytical data: Calcd for $C_{43}H_{30}N_{10}Ru$: C, 65.55; H, 3.84; N, 17.78. Found: C, 65.56; H, 3.83; N, 17.77%. ^{1}H NMR (DMSO-d_6, 400 MHz): δ 9.29 (d, 3H), 9.26 (d, 2H), 9.14 (d, 3H), 8.90-8.84 (m, 5H), 8.50-8.44 (m, 4H), 8.22 (s, 2H), 8.20 (m, 2H), 8.08 (s, 1H), 7.84 (m, 2H), 7.61 (t, 2H), 7.88 (d, 2H), 7.37 (m, 2H), 7.33 (d, 2H); ^{13}C[^{1}H] NMR (100, MHz, DMSO-d_6): δ 157.84, 156.77, 156.54, 154.51, 151.54, 151.39, 149.99, 137.89, 135.40, 132.32, 130.50, 127.79, 129.90, 127.71, 127.27, 124.48; IR (KBr): 3575 (υ, N-H), 2923 (υ, C-H), 1089 (υ, C-N), 1556 (ϑ, C=N) 1740 (υ, C=C), 623 cm^{-1} (υ, Ru-N).

Synthesis of $[Ru(dmb)_2(NPPIP)](ClO_4)_2.2H_2O$ (3)

The $[Ru(dmb)_2(NPPIP)]^{+2}$**(3)** was prepared by following complex-1 procedure by adding a mixture of *cis*-$[Ru(dmb)_2Cl_2]\cdot 2H_2O$ (0.5 mmol, 0.288 g) and NPPIP ligand (0.5 mmol, 0.187g) was dissolved in ethanol (15 mL). Analytical data: Calcd for $C_{47}H_{38}N_{10}Ru$: C, 66.59; H, 4.54; N, 16.60. Found: C, 66.58; H, 4.56; N, 16.62%. ^{1}H NMR (DMSO-d_6 ,400 MHz): δ 9.29 (d, 3H), 9.25 (d, 3H), 9.10 (s, 1H), 9.08 (m, 2H), 8.75 (d, 3H), 8.41 (m, 3H), 8.27 (m, 2H), 8.18 (m, 2H), 8.08 (m, 1H), 7.93 (d, 2H), 7.67 (d, 2H), 7.16 (m, 2H), 2.55-2.46 (s, 12H); ^{13}C[^{1}H] NMR (100, MHz, DMSO-d_6): δ 157.57, 156.34, 154.59, 151.56, 149.70, 132.45, 128.63, 127.82, 127.39, 125.08; IR (KBr): 3589 (υ, N-H), 2925 (υ, C-H), 1073 (υ, C-N), 1625 (υ, C=C), 623 cm^{-1} (υ, Ru-N).

Biophysical study of DNA binding affinity of Ru(II) polypyridyl complexes

The DNA binding studies of Ru(II) complexes were studied using Biophysical methods - Absorption, Fluorescence, Quenching, DNA cleavage and viscosity methods.

DNA - binding by electronic absorption studies

The DNA binding affinities were measured *via* absorption titrations by increasing the concentration of DNA to a fixed metal complex quantity (20 µL) at RT. Ru-DNA solutions were incubated (for 5 min) before recording the absorption spectra. Equation 1 was used to derive the intrinsic binding constants, K_b[34].

$$[DNA]/(\varepsilon_a - \varepsilon_f) = [DNA]/(\varepsilon_b - \varepsilon_f) + 1/K_b(\varepsilon_b - \varepsilon_f) \quad \ldots (1)$$

Where, ε_a, ε_f, and ε_b represent the noticeable absorption extinction coefficient (A_{obsd} / [complex]), the extinction coefficient of the complex in the fully bound form, and the extinction coefficient of the free complex, respectively and [DNA] is the concentration of DNA. From the plots of [DNA]/ (ε_a-ε_f) *versus* [DNA] the binding constant K_b is given in the ratio between slope and the intercept.

Fluorescence (Luminescence) Studies

$$C_b = C_t\,[(F - F_0)/(F_{max} - F_0)] \quad \ldots (2)$$

The luminescence titrations were carried out similarly to absorption titrations using the Tris–HCl buffer. To a fixed metal concentration (20 µL), different concentrations (10-120 µL) of DNA were added. The fraction of the compound bound was calculated from equation (2), where C_t is the total complex concentration, F is the observed fluorescence emission intensity at a given DNA concentration, F_0 is the intensity in the absence of DNA, and F_{max} is when the complex is maximally bound to DNA. The fluorescence binding constant (K_b) of complexes 1 and 2 was obtained from the Scatchard equation, and data were cast into the Scatchard plot of r/C_f against r. Where r is the C_b / [DNA], and C_f is the concentration of the free complex[35].

Fluorescence quenching studies

The Tris-HCl buffer solution (*p*H 7.5) was employed in the fluorescence experiments. Different concentrations of the complexes (1 and 2) were added to an ethidium bromide and CT-DNA solution to allow for reaction. The concentrations of the complexes were kept between 10 and 100 µM, whereas ethidium bromide and CT DNA were kept at 130 and 40 µm, respectively. Ethidium bromide's emission range was kept between 560 and 760 nm, and its emission spectra were observed at 520 nm. By using the Stern-Volmer equation: $I_0/I=1+K_{sv}$ r, where I and I_0 Stand for flurorescence intensities in the presence and absence of complexes, respectively, and

K_{SV} linear Stern-Volmer quenching constant based on the ratio of r_{EB} (the ratio of the bound concentration of EB to the concentration of DNA) and total concentration of the complex to that of DNA, is r thus the spectra were examined.

Viscosity experiments

The Ostwald viscometer was used for the viscosity studies (maintained at a constant temperature of 29 ± 0.1°C in a thermostat water bath). Each sample's flow time was measured three times using a digital stopwatch, and the average flow time was computed. Data are displayed as $(\eta/\eta_0)^{1/3}$ *vs*. binding ratio, where η is the DNA's viscosity when the complex is present and η_0 is the DNA's viscosity when CT-DNA is used alone. The measured flow time of DNA-containing solutions (t) was used to determine the viscosity values, which were then adjusted for the observed flow time of the buffer alone (t_0) [36,37].

DNA cleavage experiment

The agarose gel electrophoresis method was employed to verify the metal complexes' capacity to cleave DNA. In this test, metal complexes were applied to supercoiled pBR322 DNA at several quantities, and then the DNA was diluted with Tris-HCl buffer at *p*H 7.2. The pretreatment DNA sample system was mixed with bromophenol blue (2L) and then incubated for a further two hours at 37°C. The samples were then loaded onto the wells of a 1% agarose gel that was set in a tray containing TAE buffer (*p*H 8.0) and electrophoresed for 45 minutes at 70 V. Before electrophoresis, the gel was treated with ethidium bromide and a BIO-RAD Gel documentation system, bands were seen under an ultraviolet (UV) Transilluminator and the gel that resulted was photographed[38,39].

Antimicrobial activity

Antimicrobial studies were performed by using the pour plate method. The complex was tested for its antimicrobial activity against Staphylococcus, Bacillus, E.coli, Klebsiella, Candida and Aspergillus. Four different concentrations (25µL, 50µL, 75µL and100µL) in DMSO were used for testing the spore germination of each fungus. In this method, 1% of active bacterial and antibiotic (Streptomycin/ Chloramphenicol) cultures were mixed into autoclaved agar media just before solidifying temperature and poured into the petri plates. After the plates were solidified, and using a sterilised well borer, samples were loaded 100µL each into the wells, followed by incubation at 37°C for 18-24 hours in a bacterial incubator and at 25°C for 96 hours in a fungal incubator. These results were compared with standard antibacterial drug streptomycin (5µg/mL) and antifungal agents Fluconazole (5µg/mL) for Candida, MancozebWp75 (5µg/mL) for Aspergillus at the same concentration.

Cytotoxicity

A standard literature 3-(4,5-dimethylthiazole)-2,5-diphenyltetrazolium bromide (MTT) assay procedure was used to evaluate *in vitro* cytotoxicity of synthesised compounds. The cells were seeded in a 96-well flat-bottom microplate and maintained at 37°C in 95% humidity and 5% CO_2 overnight. Different concentrations (100, 50, 25, 12.5, 6.25, 3.125 µg/mL) of the sample were added to the cells and incubated for 48 hours. The wells were washed twice with PBS, and 20 µL of the MTT staining solution was added to each well, and the plate was incubated at 37°C. After 4h, 100 µL of DMSO was added to each well to dissolve the formazan crystals, and absorbance was recorded at 570 nm using a microplate reader[40,41].

Formula: Surviving cells (%) = Mean OD of test compound /Mean OD of negative control × 100

Using GraphPad Prism version 5.1, we calculate the IC_{50} of the compound.

Results and Discussion

Spectroscopic Characterisation of Ru (II) Complexes

The IR bands at 803-885 cm^{-1} correspond to the C-H stretching vibrations of aromatic ring systems, while the band at 718-736 cm^{-1} represents the C-H mode of the pyridine molecule. When a complex forms, the C-H, N-H, and C-N bands move to higher frequencies. For example, the NPPIP C-H peak (803 cm^{-1}) moves to 842, 843, and 854 cm^{-1} in complexes 1, 2 and 3. C=C and C=N stretching are responsible for the additional bands at 1625-1740 cm^{-1} and 1526-1570 cm^{-1}, respectively. Ru-N is represented by a band at 623 cm^{-1}. A large N-H vibration band develops at 3887-3957 cm^{-1}.

The ^{1}H NMR spectra show significant changes in the chemical shifts of NPPIP ligand protons during complex formation. The NPPIP ligand peaks initially ranged from 7.8 to 13.9 ppm, while the 1,10-phenanthroline ligand occurred between 5.5 and 8.8 ppm, bipyridine between 5.4 and 7.2 ppm, and

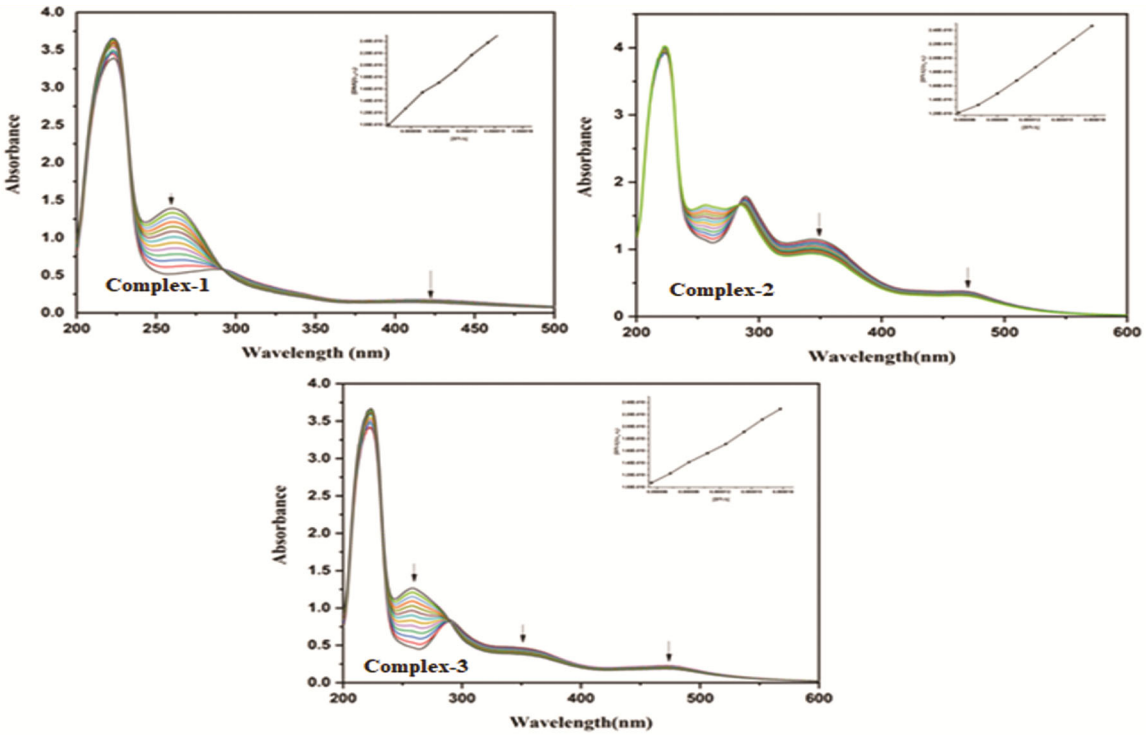

Fig. 1 — Absorption studies of Ru(II) NPPIP polylyridyl complexes in Tris-HCl buffer upon addition of CT-DNA. Arrow shows hypochromic and bathochromic shifts upon increase of DNA concentration. Inserted plot, [DNA]/(ε_a-ε_f) *versus* [DNA] for the titration of DNA with Ru(II) complex, which gives intrinsic binding constant (K_b)

dimethyl bipyridine between 3.2 and 5.8 ppm. Following complex formation, all signals migrated downfield, with protons near the N-donor atom emerging at 9.0 and 8.9 ppm, and a broad N-H peak at 7.7 ppm. The ^{13}C NMR showed shifts in carbon signals from 149.91, 147.76 ppm to 152.10, 150.10 ppm, supporting complex formation.

The interchelator ligand NPPIP adduct forms with a proton (M+H) - 375.2 to its experimental mass at 374.1. The double charged M+1 peak of $[Ru(phen)_2NPPIP]^{+2}$, $[Ru(bpy)_2NPPIP]^{+2}$ and $[Ru(dmb)_2NPPIP]^{+2}$ are at 527.1,393.9, and 422.4 respectively.

The UV-Vis electronic spectrum of NPPIP ligand and its Ru (II) complex is placed in the Supplementary Information Figure S1. The π-π* and n-π* transitions wide peak were observed at 223 nm and 290 nm owing to of NPPIP ligand. When the NPPIP ligand binds to the metal ion, in addition a new broad band appears between 410-470 nm, corresponding to visible metal-ligand charge transfer (MLCT) transitions. The $[Ru(phen)_2NPPIP]^{2+}$, $[Ru(bpy)_2NPPIP]^{2+}$and $[Ru(dmb)_2NPPIP]^{2+}$ complex has shown a maximum at 410, 464 and 470 nm, respectively (Supplementary Information Figure S1).

Biophysical Study of DNA Binding Affinity of Ru(II) Polypyridyl Complexes

UV-Visible studies of NPPIP-based complexes

Absorption studies of the synthesized Ru(II) complexes with DNA, shown in Fig. 1 reveal spectral changes (with hypochromism (H%) and bathochromism) indicative of intercalation binding. Bands below 300 nm are attributed to intra ligand (IL) pπ-pπ transitions, while those in the visible region correspond to metal-to-ligand charge transfer (MLCT) transitions. The intrinsic binding constants (K_b) of complexes 1, 2, and 3 were determined by monitoring the decrease in absorbance at the MLCT band as DNA was added. The results show that all complexes exhibit strong DNA binding, with complex 1 showing the highest affinity, followed by complexes 2 and 3. This stronger binding is attributed to the increased planarity of the ancillary phen ligand. In contrast, methyl substitutions at the 4, 4'-positions of the dmb ligand introduce steric hindrance, reducing the binding constant. The K_b values follow the order: (1) > (2) > (3) (Table 1).

Fluorescence emission studies

The metal complexes' binding strength to CT-DNA was determined using fluorescence emission

Table 1 — Binding constants of Ru(II) NPPIP complexes

S. No.	Complex	K_b (M^{-1}) (Absorption)	K_b(M^{-1}) (Emission)	K_{sv} value
1	$[Ru(phen)_2(NPPIP)]^{+2}$	2.5×10^5	7.2×10^6	9.2×10^3
2	$[Ru(bpy)_2(NPPIP)]^{+2}$	1.6×10^5	6.9×10^6	9.1×10^3
3	$[Ru(dmb)_2(NPPIP)]^{+2}$	1.5×10^5	6.2×10^6	1.8×10^4

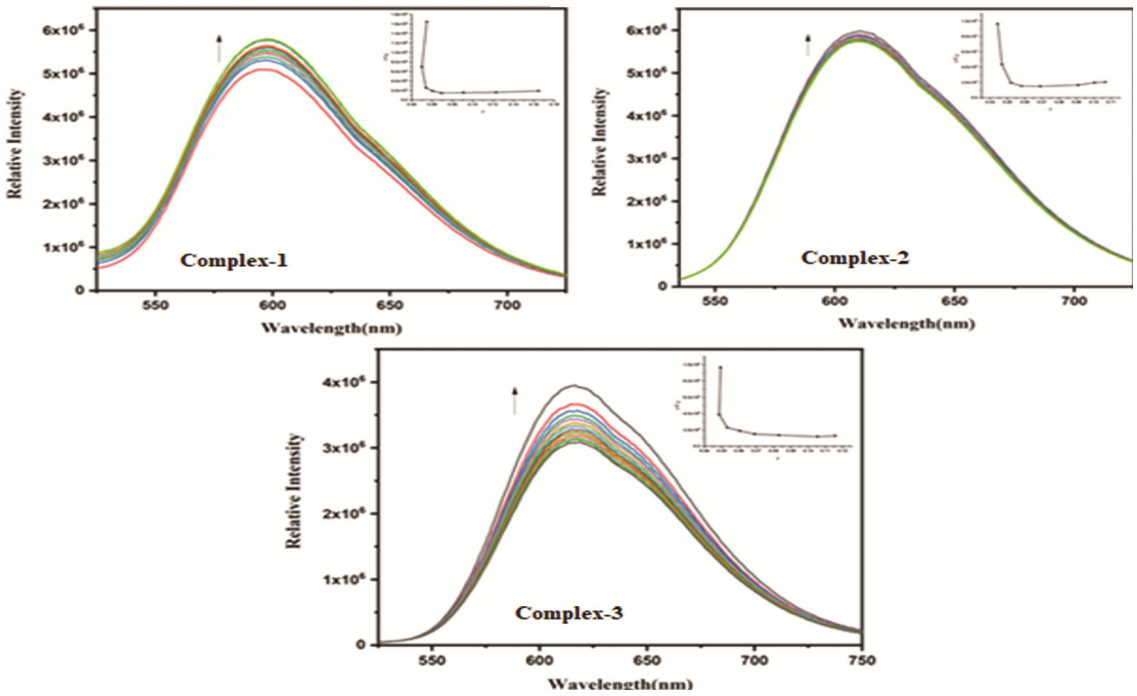

Fig. 2 — Fluorescence emission studies spectra of Ru(II) NPPIP polypyridyl complexes in Tris-HCl buffer upon addition of CT-DNA. The arrow shows the intensity changes upon the increase of DNA concentration. Inset: Scatchard plot of above complexes, which gives binding constant (K_b)

titrations, a sensitive approach for evaluating drug-DNA interactions (Fig. 2). The complexes were stimulated at 410, 464 and 470 nm, and emissions were detected at 595, 610 and 617 nm, respectively. As the concentration of CT-DNA grew, so did the strength of the emissions, which eventually plateaued. The binding constant was estimated using a modified Scatchard equation, and the intrinsic binding constants (K_b) were calculated using Scatchard plots (r/C_f *vs*. r).The K_b values for complexes 1, 2, and 3 were found to be 7.2×10^6 M^{-1}, 6.9×10^6 M^{-1} and 6.2×10^6 M^{-1}, respectively (Table 1). The variation in K_b values is attributed to differences in the ancillary ligands. Complex 3 exhibits a lower K_b value due to the steric hindrance.

Fluorescence quenching studies

The two DNA groove binders and intercalators can diminish fluorescence intensity, with intercalators such as ethidium bromide (EB) having a considerable effect. Fluorescence quenching tests with EB were carried out to study the complexes' intercalative binding mechanism to CT-DNA. Emission intensity increases as EB intercalates into DNA (Fig. 3). In this investigation, a solution with 40 µM EB and 130 µM CT-DNA was titrated with increasing concentrations of the complex (10-100 µM), resulting to a decrease in fluorescence intensity. The Stern-Volmer equation shows that the complexes bind to CT-DNA and displace EB, indicating an intercalative binding mechanism.

The Stern-Volmer constants (Ksv) were determined from the linear fit of the plot of I_0/I *versus* [complex]/[DNA], yielding values of 9.2×10^3, 9.1×10^3, and 1.8×10^4 for complexes 1, 2, and 3 respectively (Table 1).

Viscosity studies

Viscosity tests were performed to investigate the complexes' binding mechanisms with CT-DNA.

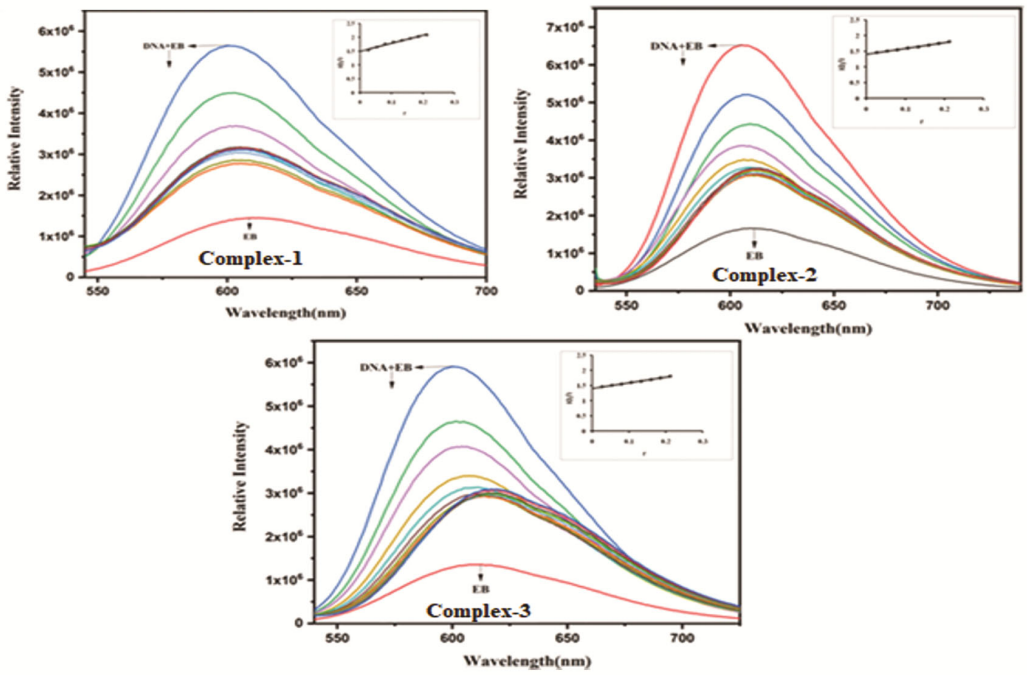

Fig. 3 — Fluorescence quenching studies spectra of Ru(II) NPPIP complexes in Tris-HCl buffer of DNA-EB complex [DNA(130 mM) and EB(40 mM)] system, with the addition of complex arrow shows the decreasing emission intensity by increasing the concentration of complex (10-100 mM), Insert: I_o/I verses r

These hydrodynamic studies are critical for understanding how ligand insertion between DNA base pairs influences DNA length and stiffness. Intercalating ligands, such as the complexes investigated, enter between base pairs to lengthen the helix and increase the viscosity of the solution. According to the traditional intercalation concept, this binding increases viscosity by separating DNA base pairs to accommodate the ligand. The results were identical to those obtained with ethidium bromide (EtBr), a well-known intercalator. As the quantity of metal complexes grew, DNA lengthened, causing the viscosity to increase. The viscosity ordering was EtBr > 1 > 2 >3, indicating an intercalation binding mode, which was validated by electronic spectroscopy and fluorescence emission measurements (Fig. 4).

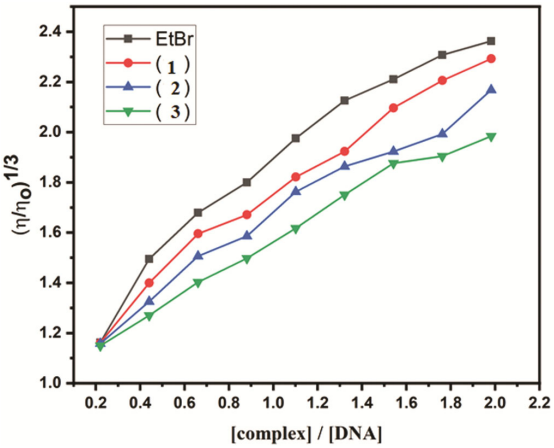

Fig. 4 — Viscosity studies of Ru(II) NPPIP complexes in Tris-HCl buffer with increasing concentration of complex and EtBr on the relative viscosity of CT-DNA at RT

Photo cleavage

The nuclease activity of the Ru(II) complex was determined using pBR322 DNA and agarose gel electrophoresis. Plasmid DNA electrophoresis is a quick procedure, and when the supercoiled form of the DNA is intact, it migrates in form I. When a nick or single-strand break occurs, the DNA relaxes into an open circular shape (form II), which moves more slowly. If both strands are broken, the DNA becomes linear (form III) and moves between forms I and II. The photolysis experiment involved incubating pBR322 DNA with the Ru(II) complex (20 µM) and then exposing it to UV light at 365 nm for 60 minutes. The absence of the metal complex resulted in no DNA cleavage, as illustrated in lane 1. However, with the addition of the Ru(II) complex, the amount of form I gradually decreased, while form II increased, as illustrated in the Fig. 5.

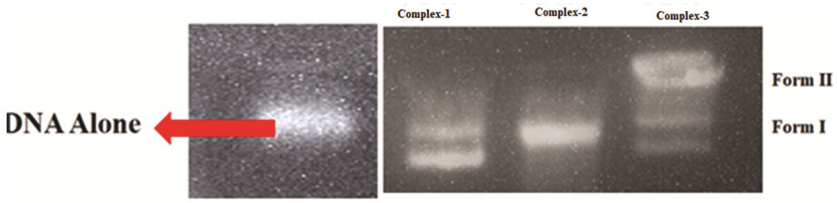

Fig. 5 — Photo cleavage images of Ru(II) NPPIP complexes in agarose gel electrophoresis of pBR322 DNA alone and in the presence of complex with the concentration range of 20 μM after irradiation at 365 nm for 60 min under UV light

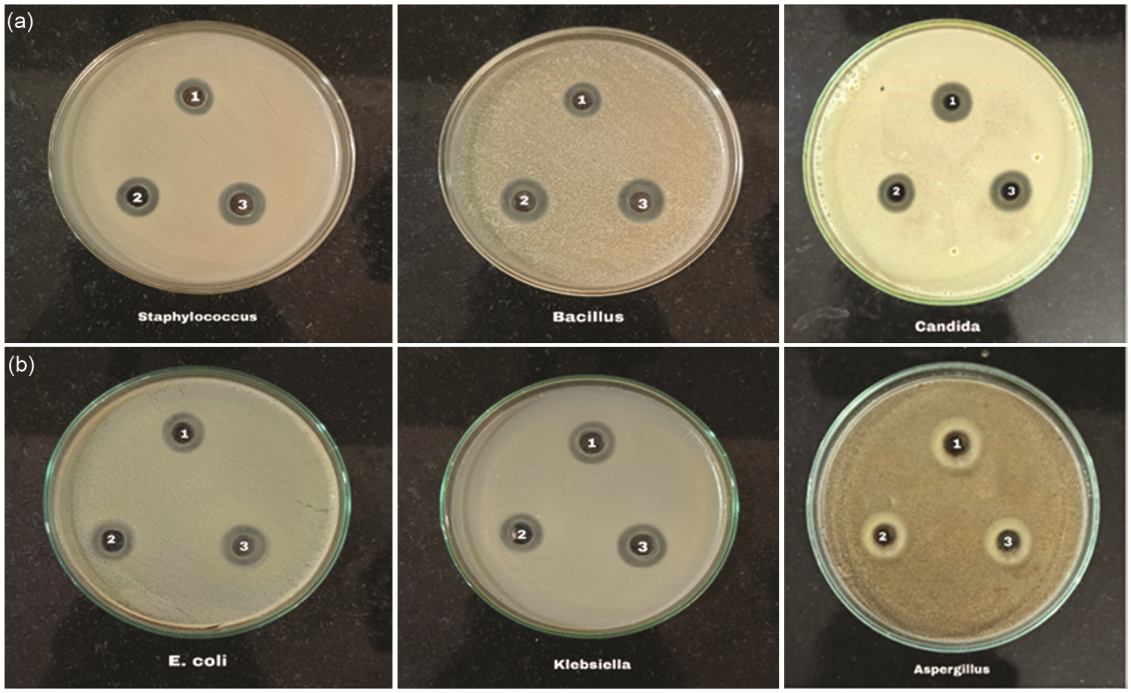

Fig. 6 — **A-**Antibacterial activity**, B-**Antifungal activity of Ru(II) NPPIP complexes

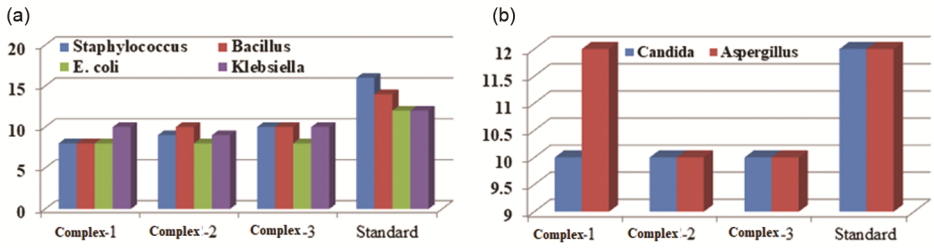

Fig. 7 — **A-**Antibacterial activity**, B-**Antifungal activity of Ru(II) NPPIP complexes

Antimicrobial Activity

The biological activity of the ligand NPPIP and its three Ru(II) polypyridyl complexes was evaluated against four bacteria: Gram-negative (E. coli, Klebsiella) and Gram-positive (Staphylococcus, Bacillus) (Fig. 6A, Fig. 7A). Complexes 1, 2, and 3 were tested for *in vitro* antibacterial activity at concentrations of 75 μL and 100 μL using the pour plate method. The antibacterial activity, measured by inhibition zones (in mm) (Supplementary Information Table S2, S3), increased with higher concentrations, with the complexes showing stronger activity against Gram-positive bacteria compared to Gram-negative, though less effective than the standard drug ampicillin. The metal complexes demonstrated significantly higher activity than the free ligand. The lowest MIC value, indicative of more efficient antimicrobial activity, was observed for complex 1 (1.4-1.5 μg/mL). In antifungal tests, complexes 1 and 2 showed notable activity against Aspergillus at

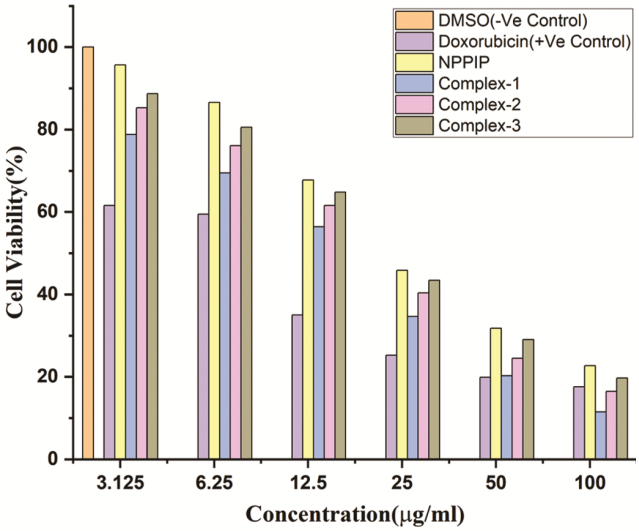

Fig. 8 — Cell Viability of MCF-7(Human breast cancer) cell line *in vitro* treatment with Doxorubicin (positive control) and Ru (II) complexes 1-3.Every data point is the average ± standard error derived from a minimum of three separate experiments. Negative control (untreated cells) considered as 100% of viable cells

Table 2 — Cytotoxicity of NPPIP ligand and its Ru(II) complexes (1-3) and Doxorubicin (positive control) on MCF-7 cell lines

S.No.	Ligand/ Ru(II) Complex	IC50 (μg/mL)
1	NPPIP ligand	44.79±0.486
2	[Ru(phen)2NPPIP]+2	25.42±0.142
3	[Ru(bpy)2NPPIP]+2	32.37±0.196
4	[Ru(dmb)2NPPIP]+2	39.33±0.258
5	Doxorubicin	3.66 ±0.07

concentrations of 50 µL and 75 µL, with inhibition zones compared to the standard (Fig. 6B, Fig. 7B).

Cytotoxicity

The antiproliferative properties of the Ru(II) complexes against MCF-7 (human breast cancer) cells were determined using the MTT test, with doxorubicin serving as a positive control. The Ru(II) polypyridyl complexes showed strong anticancer activity against the MCF-7 cancer cell line. DMSO served as a negative control. Following 48 hours of treatment with complexes 1, 2, and 3 at doses ranging from 3.125 to 100 µg/mL, the percentage suppression of cancer cell growth was measured. The cytotoxicity of the complexes was discovered to be concentration-dependent, with cell viability decreasing as the concentration increased (Fig. 8). The Ru(II) complexes exhibited significant activity against MCF-7 cells, with IC_{50} values of 25.42±0.142 µg/mL for complex 1; 32.37 ± 0.196 µg/mL for complex 2 and 39.33 ± 0.258 µg/mL for complex 3, while standard doxorubicin showed an IC_{50} of 3.66 ± 0.07 µg/mL (Table 2). Complex 1 exhibited higher cell viability compared to complexes 2 and 3, as shown in the Fig. 8. These complexes demonstrate strong inhibitory effects on the growth of MCF-7 cells and may hold potential as effective anticancer agents for breast cancer treatment.

Conclusion

The Ru(II) polypyridyl complexes of NPPIP ligand were synthesised, characterised, and their interaction with CT-DNA was studied. The viscosity, fluorescence, and absorption measurements show that all three complexes strongly intercalate with DNA base pairs, assisted by the NPPIP ligand. Complexes 1 and 2 exhibit greater DNA binding than complex 3, most likely because to the presence of unsubstituted bpy and phen auxiliary ligands in complexes 1 and 2. In contrast, complexes containing methyl modifications have a lower binding affinity due to steric hindrance. The binding affinity is in the following order: 1 > 2 > 3. The complex's antibacterial activity, measured at different concentrations, reveals remarkable efficacy against both gram-positive and Gram-negative bacteria. The chemical and biological features of the complexes are significantly influenced by the accessory ligand used, which in turn impacts their antibacterial activity. This work identifies Ru(II)-NPPIP complexes as potential antibacterial and antifungal drugs. The invitro cytotoxicity of Ru(II) polypyridyl complexes show promising anticancer activity against cell line MCF-7.Complex 1 binds DNA strongly and is also a more effective cytotoxic agent for cancer cells.

Supplementary Information

Supplementary information is available in the website https://nopr.niscpr.res.in/handle/123456789/58776.

Acknowledgement

The authors MN and NN are thankful to the Head, Department of Chemistry and the Principal, University College of Science, Saifabad, Osmania University, and the Head, Department of Chemistry and the Principal, University College of Science, Tarnaka, Osmania University, Hyderabad for the facilities to carry out this work. The authors are thankful to the DST FIST, New Delhi for the facility of the Computational Lab at Department of Chemistry, University College of Science, Saifabad, Osmania University.

Conflicts of Interest

There are no conflicts of interest to declare.

References

1 Zhang C, Xu C, Gao X & Yao Q, *Theranostics*, 12 (2022) 2115.
2 Oun R, Moussa Y E & Wheate N J, *Dalton Trans*, 47 (2018) 6645.
3 Clarke M J, *Inorganic Chemistry in Biology and Medicine*, *Ch. 10*, (American Chemical Society, US), 1980, p 157–180.
4 Storr T, *Ligand Design in Medicinal Inorganic Chemistry*, (John Wiley & Sons Incorporated), 2014.
5 Shen J, Kim H C, Wolfram J, Mu C, Zhang W, Liu H, Xie Y, Mai J, Zhang H, Li Z, Guevara M, Mao Z W & Shen H, *Nano Lett*, 17 (2017) 2913.
6 Vos J G & Kelly J M, *Dalton Trans*, (2006) 4869
7 Marin V, Holder E, Hoogenboom R & Schubert U S, *Chem Soc Rev*, 36 (2007) 618
8 Daniel C, *Coord Chem Rev*, 19 (2015) 282.
9 Fantacci S & De Angelis F, *Coord Chem Rev*, 255 (2011) 2704.
10 Paris J P & Brandt W W, *J Am Chem Soc*, 81 (1959) 5001.
11 Chen T, Liu Y, Zheng W J, Liu J & Wong Y S, *Inorg Chem*, 49 (2010) 6366.
12 Toledo J C, Neto B D S L & Franco D W, *Coord Chem Rev*, 249 (2005) 419.
13 Pongratz M, Schluga P, Jakupec M A, Arion V B, Hartinger C G, Allmaier G, Keppler B K, *J Anal At Spectro*, 19 (2004) 46.
14 Yang J, Bhadbhade M, Donald W A, Iranmanesh H, Moore E G, Yan H & Beves J E, *Chem Comm*, 51 (2015) 4465.
15 Gill M R & Thomas J A, *Chem Soc Rev*, 41 (2012) 3179.
16 Pages B J, Ang D L, Wright E P & Aldrich-Wright J R, *Dalton Trans*, 44 (2015) 3505.
17 Burke C S, Byrne A & Keyes T E, *Advances in Imaging and Sensing*, *Ch. 11*, (CRC Press, Florida, USA), 2016, p. 227.
18 Cook N P, Torres V, Jain D & Martı A A, *J Am Chem Soc*, 133 (2011) 11121.
19 Thota S, Rodrigues D A, Crans D C & Barreiro E J, *J Med Chem*, 61 (2018) 5805.
20 Gao F, Chao H & Fetal Z, *J Inorg Bio Chem*, 100 (2006) 1487.
21 Vyas N A, Ramteke S N, Kumbhar A S, Kulkarni P P, Jani V, Sonawane U B, Joshi R R, Joshi B & Erxleben A, *Eur J Med Chem*, 121 (2016) 793.
22 Cook N P, Torres V, Jain D & Marti A A, *J Am Chem Soc*, 133 (2011) 11121.
23 Liu J, Mei W J, Lin L J, Zheng K C, Chao H, Yun F C & Ji L N, *Inorg Chem Acta*, 357 (2004) 285.
24 Trondl R, Heffeter P, Kowal C R, Jakupec M A, Berger W & Keppler B K, *Chem Sci*, 5 (2014) 2925.
25 Clarke M J, *Coord Chem Rev*, 236 (2003) 209.
26 Dwyer F P, Reid I K, Shulman A, Laycock G M & Dixson S, *Aust J Exp Biol Med Sci*, 47 (1969) 203.
27 Dwyer F P, Gyarfas E C, Rogers W P & Koch J H, *Nature*, 170 (1952) 190.
28 Bolhuis A, Hand L, Marshall J E, Richards A D, Rodger A, Wright J A, *Eur J Pharm Sci*, 42 (2011) 313.
29 Srishailam A, Kumar Y P, Gabra N M D, Reddy P V, Deepika N, Veerababu N & Satyanarayana S, *J Fluoresc*, 23 (2013) 897.
30 Salvà-Serra F, Gomila M, Svensson-Stadler L, Busquets A, Jaén-Luchoro D, Karlsson R & Moore E R, *Imp Prot Exch*, (2018), https://doi.org/10.1038/ protex.2018.084.
31 Vijayalakshmi R, Kanthimathi M, Subramanian V & Nair B, *Biochim Biophys Acta*, 1475 (2000) 157.
32 Zheng R H, Guo H C, Jiang H J, Xu K H, Liu B B, Sun W L & Shen Z Q, *Chinese Chem Lett*, 21 (2010) 1270.
33 Goss CA & Abruna H D, *Inorg Chem*, 24 (1985) 4263.
34 Wolfe A, Shimer G H & Meehan T, *Biochem*, 26 (1987) 6392.
35 McGhee J D, Von Hippel P H, *J Mol Bio*, 86 (1974) 469.
36 Satyanarayana S, Dabrowiak J C & Chaires J B, *Biochem*, 32 (1993) 2573.
37 Satyanarayana S, Dabrowiak J C & Chaires J B, *Biochem*, 31 (1992) 9319.
38 Long E C & Barton J K, *Acc Chem Res*, 23 (1990) 271.
39 Barton J K & Raphael A L, *J Am Chem Soc*, 106 (1984) 2466.
40 Anupama B, Aruna A, Manga V, Sivan S, Sagar M V & Chandrashekar R, *J Fluoresc*, 27 (2017) 953.
41 Vuradi R K, Nambigari N, Pendyala P, Gopu S, Kotha L R, Deepika G, Vinoda R M & Sirasani S, *App Organomet Chem*, 34 (2020) e5332.